Pakistan Veterinary Journal

ISSN: 0253-8318 (PRINT), 2074-7764 (ONLINE)
DOI: 10.29261/pakvetj/2026.007

RESEARCH ARTICLE

Multidimensional Evaluation of Artemisinic Acid Against Colitis in Murine Model: Integrating Microbiota Remodeling, Histopathological Improvement and Inflammation Regulation

Ling Wang[1,#], Xiaohong Zheng[1,2,#], Muhammad Shoaib[3,*], JiongJie He[1,*], Amjad Islam Aqib[4], Wenzhu Guo[1], YuzhangYan[1,2], Xingqian Zhou[1], Saad Ahmad[1], and Shengyi Wang[1,*]

[1]Key Laboratory of New Animal Drug Project, Gansu Province; Key Laboratory of Veterinary Pharmaceutical Development, Ministry of Agriculture and Rural Affairs; Lanzhou Institute of Husbandry and Pharmaceutical Sciences of Chinese Academy of Agricultural Sciences, Lanzhou 730050, China; [2]College of Animal Science and Technology, Guangxi University, Nanning 530005, China; [3]Jiangsu Co-Innovation Center for Prevention and Control of Important Animal Infectious Diseases and Zoonoses, College of Veterinary Medicine, Yangzhou University, Yangzhou 225009, China; [4]Department of Medicine, Cholistan University of Veterinary and Animals Sciences, Bahawalpur 63100, Pakistan.
#These authors contributed equally to this study.
*Corresponding author: shoaibsinko8@gmail.com; ajie@163.com; wangshengyi@caas.cn

ARTICLE HISTORY (25-1142)

Received: November 22, 2025
Revised: December 19, 2025
Accepted: December 23, 2025
Published online: January 22, 2026

Key words:
16S rRNA sequencing
Artemisinic acid
Histopathology
Inflammatory cytokines
Intestinal microbiota

ABSTRACT

Colitis is a chronic inflammatory bowel disease (IBD) that poses a potential threat to animal health and requires effective treatment options. The artemisinic acid (AA), a sesquiterpene compound in alleviating the colitis is least studied. In this study, we investigated the effect of AA on dextran sodium sulfate (DSS) induced colitis in mice model. Thirty-seven mice were randomly divided into six groups of negative control (NC), model (DSS), three treatments (L, 0.10mg/g; M, 0.20mg/g; H, 0.40mg/g), and positive control (LH, 0.01mg/g). Each group having six mice except DSS that had seven mice. The results showed that the body weight of all DSS-treated groups decreased significantly ($P<0.001$) compared to NC group. The colon length of DSS group was shortened significantly compared to NC and H groups ($P<0.01$). The disease activity index of DSS-treated group was increased significantly compared to NC group ($P<0.001$) but significantly improved with H, M, and L doses. Histopathological analysis revealed significant improvement in all treatment groups compared to DSS group. Compared with DSS group, the levels of IL-6, IL-10 and IFN-γ in the H, M, and L treatment groups decreased significantly ($P<0.001$). The DSS-induced colitis resulted in imbalance of gut microbiota in terms of pathogenic species while AA resulted in increase of relative abundance of beneficial bacteria such as *Lactobacillus*. Thus study concludes that AA has the potential to alleviate colitis by improving intestinal morphology, regulating inflammatory factors, and restoring beneficial intestinal microbiota. Therefore, this compound may offer a promising therapeutic approach to treat colitis in animals.

To Cite This Article: Wang L, Zheng X, Shoaib M, He J, Aqib AI, Guo W, Yan Y, Zhou X, Ahmad S, and Wang S, 2026. Multidimensional evaluation of artemisinic acid against colitis in murine model: integrating microbiota remodeling, histopathological improvement and inflammation regulation. Pak Vet J. http://dx.doi.org/10.29261/pakvetj/2026.007

INTRODUCTION

Colitis is a chronic inflammatory bowel disease (IBD) which is recognized as ulcerative colitis (UC) in humans and chronic enteropathy (CE) in veterinary (Froushani *et al*., 2025; Ma *et al*., 2025). Although the exact etiology of IBD is unknown, studies have found close association among genetic, environmental, and gut microbial dysbiosis. However, multiple other factors such as stress, food and drug allergies also contribute to the occurrence of colitis in dogs and cats. Currently, it is believed that the intestinal microbiota imbalance is an important driver for the occurrence and development of IBD (Xie *et al*., 2024). IBD further disturbs the gut microbial balance, negatively influencing immune and metabolic processes and contributing to disease progression (Zhang *et al*., 2022). The treatment of colitis can include anti-inflammatory and antimicrobial drugs along with managing other factors. Due to the development of antimicrobial resistance, complementary and alternative therapies including

probiotics, prebiotics, and natural compounds are of great significance. Studies have shown that traditional chinese medicine can alleviate intestinal inflammation by improving intestinal mucosal damage, inhibiting pro-inflammatory cytokine levels, and restoring intestinal flora homeostasis (Huang *et al.*, 2024; Wang *et al*., 2025; Zhu *et al*., 2025).

Artemisinin (ART) and artemisinic acid (AA) are sesquiterpenoids produced from *Artemisia annua* L. belong to *Asteraceae* family. They share some similarities such as part of biosynthetic pathway and derived from same terpene precursor. However, ART contains endoperoxide bridge (—O—O—) while AA contains carboxylic acid group. Moreover, AA act as synthetic precursor of artemisinin, which has antimalarial, antibacterial, antipyretic, anti-tumor, and synergistic effect on the antimalarial activity of artemisinin (Addissouky, 2025). Previous study has evaluated the efficacy of ART with Qinghao powder against *Eimeria tenella* and found significant reduction in the number of fecal oocystis in infected chickens, and alleviated intestinal lesions and damage without significant toxic side effects (Wang *et al*., 2021). Another study found that the in vivo antibacterial activity of artemisinin and its derivatives is mainly associated with anti-inflammatory activity of these drugs, while in vitro studies mostly focused on the modulation effect of the antibiotics (Ul Haq *et al.*, 2022). Due to the efficient killing effect of ART against *Plasmodium falciparum*, other co-existing chemical components such as AA are often ignored (Ain *et al*., 2024). A study by Liao *et al*. (2021) has shown that these co-existing components have many pharmacological activities that cannot be ignored, such as antipyretic, anti-inflammatory, antibacterial, anti-asthma, anti-oxidation, and anti-tumor.

Currently, the studies are scarce on the direct effect of AA in alleviating the colitis by regulating inflammatory cytokines and intestinal flora. In recent years, high-throughput sequencing has developed rapidly, which can immediately reveal the diversity and formation of microbial communities in the in-situ environment (Johnson *et al*., 2019). In this study, we explored the effects of AA on colitis induced by dextran sodium sulfate (DSS) in murine model through intestinal histopathology, anti-inflammatory cytokines, and 16S rRNA sequencing.

MATERIALS AND METHODS

Experimental design: Thirty-seven specific pathogen free (SPF)-grade BALB/c mice (16.72±1.09g, female, aged 7-8 weeks) were obtained from the Laboratory Animal Center of Lanzhou Veterinary Research Institute of CAAS, and acclimatized for at least 7 days under standard housing and feeding conditions. Dextran sulfate sodium (DSS, 40,000Da, Shanghai Bide Pharmaceutical Technology Co., Ltd, China) was used for the induction of colitis through oral route. The total experimental design comprised of 17 days as summarized in Fig. 1. Briefly, after first week, the mice were randomly divided into six groups [n=6 mice each except DSS model group (n=7)]. During the 8-13 days period, 3-5% DSS (w/v, 3% DSS from 8-9 days, 5% DSS from 10-13 days) was used to induce the acute colitis in mice except NC group. From day 14 to 16, normal control (NC) and model group (DSS) were treated with sterile water; treatment groups [low-dose (L), 0.10mg/g BW/day; medium-dose (M), 0.20mg/g BW/day; high-dose (H), 0.40mg/g BW/day)] with AA (purity ≥98%) by dissolving in sterile water for oral gavage (*ig*) once a day; positive control (LH) with Loperamide Hydrochloride (Xian Janssen Pharmaceutical Ltd., China) at dose rate of 0.01mg/g BW/day (*ig*). The behavior, body weight (BW), diarrhea, and bloody stools of the mice were observed, weighted and recorded daily during experimental period. After 24h (day 17) of last treatment, all animals were euthanized, the colon tissue was collected and its length was measured, the fecal contents were collected and stored for further analysis.

Disease activity index (DAI) score: Disease activity index (DAI) scoring was conducted during 8th to 16th day on daily basis for all mice referring to previous study (Luo *et al*., 2024). The disease severity of the DSS induced mice was evaluated by relying on comprehensively scoring of weight loss (%), stool characteristics and morphology, as well as the state of hematochezia. Fecal occult blood test was performed using the urine fecal occult blood test kit (Yeasen Biotechnology, Shanghai, China).

Histopathological analysis of colon and serum inflammatory cytokine assay: Tissues of colons were fixed and preserved by neutral buffered formalin solution (10%) for histopathological examination after Hematoxylin and Eosin (H&E) staining. The histopathological damage and the extent of inflammatory infiltration, histopathological changes in crypt structure, ulceration and crypt loss, ulcer, and presence or absence of edema were assessed (Liu *et al*., 2020). The pro-inflammatory cytokines such as interleukin (IL)-1β, IL-6, IL-10, and interferon (IFN)-γ were measured in the serum by ELISA kits (Shanghai Enzyme-linked Biotechnology Co., Ltd. China) according to the manufacturer's protocol.

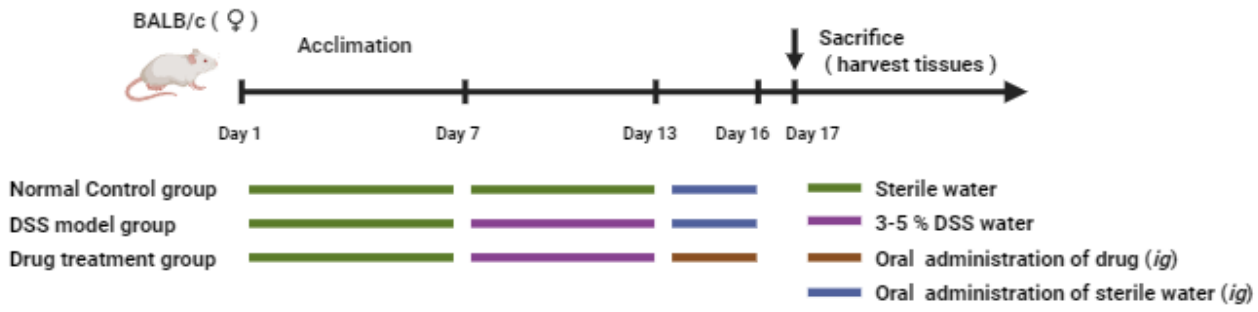

Fig. 1: The experimental design of current study for drug intervention in mouse model.

16S rRNA sequencing and bioinformatics analysis: The total DNA of mouse fecal contents was extracted and highly variable V3-V4 region of bacterial 16S rRNA gene was amplified by PCR using universal primes 338F (5′-ACTC CTAC GGGA GGCA GCAG-3′) and the reverse sequencing primer 806R (5′-GGAC TACH VGGG TWTC TAAT-3′) (Wei *et al.,* 2023). The product was purified, quantified and homogenized to prepare sequencing libraries. Finally, the sequencing was done on the Illumina MiSeq and bioinformatics analysis was done using the Majorbio cloud platform (https://cloud.majorbio.com) and various bioinformatics tools such as fastp v.0.19.6 for quality filtration, Uparse v.7.0.1090 for sequence clustering into operation taxonomic units (OTUs), Fasttree v.2.1.3 for phylogenetic tree construction, and Networkx v.1.11 for co-occurrence network analysis.

Statistical analysis: The data were analyzed using one-way analysis of variance (ANOVA), followed by Dunnett-t post-hoc test (SPSS Statistics 19.0, IBM, Chicago, IL, USA) considering 5% probability. Graphs were drawn through GraphPad Prism 8.0 (GraphPad Prism, San Diego, CA, USA).

RESULTS

Effects of AA on body weight, colon length, and DAI: DAI score reached the highest value on the 13th day, and the results of all groups were consistent. After the second day of DSS treatment, except NC group, the body weight (BW) of DSS-treated mice in the other groups began to decline, and the degree of body mass decline was relatively consistent. After the use of DSS was stopped following the 14th day and drug treatment for 3 days, the BW of mice in all drug-treated groups and DSS model group recovered significantly, and the BW recovery was the most ideal in the M group, followed by L, H, LH, and DSS groups (Fig. 2a). The results showed that the DSS-treated mice showed obvious symptoms of acute colitis, which were relieved after the administration of AA and LH. H, M, and L doses of AA could improve the decrease of BW loss induced by DSS ($P<0.01$). Compared with DSS model group, DAI score of mice in high-, medium-, and low-dose groups was significantly decreased after 3 days of treatment ($P<0.01$) (Fig. 2b). Compared with NC group, the DSS group had a significantly shorter colon length ($P<0.01$). There was no significant difference between the high-, medium-dose groups of AA and the NC group ($P>0.05$). The colon length difference between the DSS model group and M, L, and LH groups was not significant (Fig. 2c).

Effects of AA on histopathology of colon: The NC group had clear and visible layers of colon tissue, complete and continuous mucosal epithelium, and glandular cells arranged in an orderly manner within the crypt, with no infiltration of inflammatory cells and no ulceration observed (Fig. 3). The colon tissue in DSS group mice showed visible pathological damage, mucosal shedding,

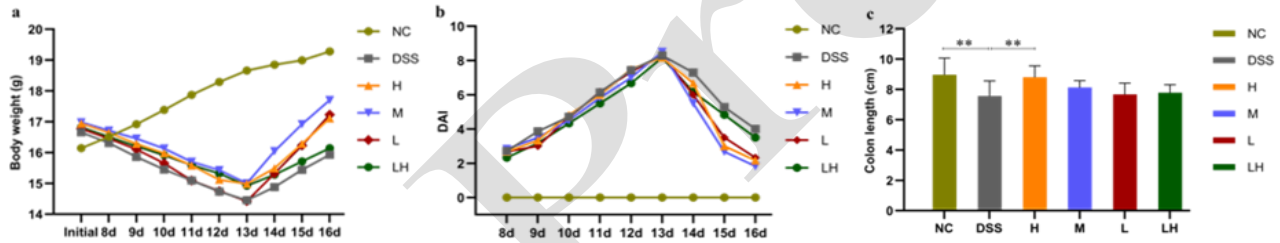

Fig. 2: Effects of AA on (a) body weight, (b) DAI, and (c) colon length in DSS-induced colitis mice. The values are presented as mean±SD. The levels of significance are indicated as; *P<0.05, **P<0.01, and ***P<0.001.

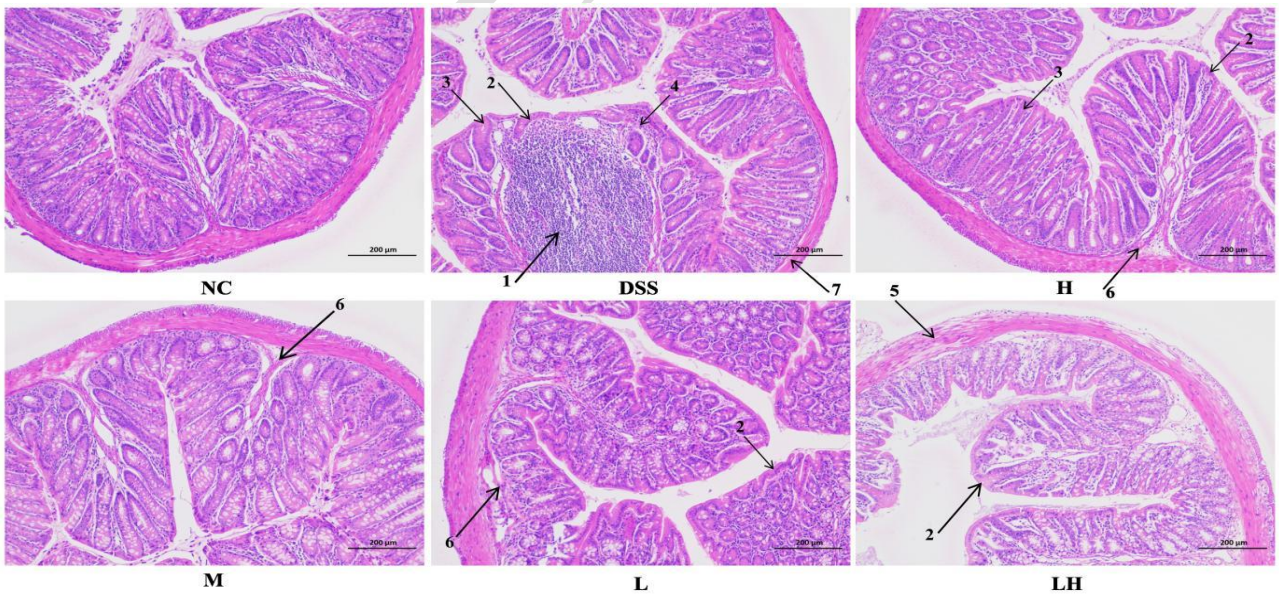

Fig. 3: Histopathological changes in colon tissue of each group done by Hematoxylin & Eosin staining (H&E, ×100). Histopathological lesions are marked with arrows and numbered for demarcation such as 1=ulceration and infiltration of inflammatory cells; 2=mucosal shedding; 3=goblet cell loss; 4=inflammatory cells; 5=stratification of muscle layers and mucosal tissue not clear; 6=congestion; 7=thin muscle layer.

significant edema of mucosal layer structure, incomplete mucosal epithelial cells, and typical ulcerative inflammatory lesions. The colon tissues of the DSS model group and each drug treatment group were accompanied by a certain degree of goblet cell loss, congestion, and mucosal damage. Compared with the DSS group, the colon injury of mice in each drug treatment group was significantly reduced, and the mucosal tissue structure was relatively intact. There was a small amount of inflammatory cell infiltration in the lamina propria, and no ulcers were observed. The recovery of goblet cell count in the high and medium dose groups of AA was better than that in the low dose and LH groups of AA.

Effects of AA on levels of serum inflammatory cytokines: , The levels of all cytokines in the serum of the DSS model group were increased compared with the NC group (Fig. 4a-d), however, the significant differences ($P<0.01$) were noted for IL-6, IL-10, and IFN-γ. Compared with the DSS model group, the levels of IL-6, IL-10 and IFN-γ in the H, M, and L treatment groups decreased significantly ($P<0.001$), while the levels of IL-1β differed significantly ($P<0.01$) in the H group.

Effects of AA on gut microbiota diversity and community structure: A Venn diagram analysis of 2,338 OTUs revealed distinct gut microbiota profiles across groups. The NC group contained 857 OTUs that belonged to 149 genera (Fig. 5a & 5b). The DSS model group contained 1295 OTUs, which belonged to 142 genera. The LH group contained 1379 OTUs, which belonged to 134 genera. The H group contained 1079 OTUs, which belonged to 144 genera. The M group contained 986 OTUs, which belonged to 135 genera. There were 441 OTUs shared by all five groups, which belonged to 103 genera. The NC group had 80 unique OTUs, the DSS model group had 301 unique OTUs, the positive drug LH group had 398 unique OTUs, and the H and M groups had 157 and 144 unique OTUs, respectively.

All samples were classified at the OTU level in partial least squares discriminant analysis (PLS-DA) analysis, and could be clearly distinguished and clustered into five groups, indicating significant differences in the composition of microflora in each group (Fig. 5c). The DSS samples are clustered separately and are not in the same quadrant as other samples. The samples of the LH group were also grouped separately into a cluster, which was not in the same quadrant as the other samples. The distance between the NC, H, and M groups were relatively close, and the NC and M groups were located in the same quadrant. PLS-DA analysis of the dispersion of sample points showed that DSS-induced modeling could change the microflora types of normal mice, and the microflora composition of different groups was significantly different. After the intervention of AA and LH, the effect of AA on the recovery of intestinal flora in mice was better than that of LH.

The Neutral Community Model (NCM) successfully estimated most of the relationship between OTUs frequency and its relative abundance (RA) change (Fig. 5d). The community variance for all groups was 63.82%, and the *p*-value was 0.0397, indicating that the neutral community model had a good overall fit, and the contribution of stochastic processes to community assembly was greater than that of deterministic processes.

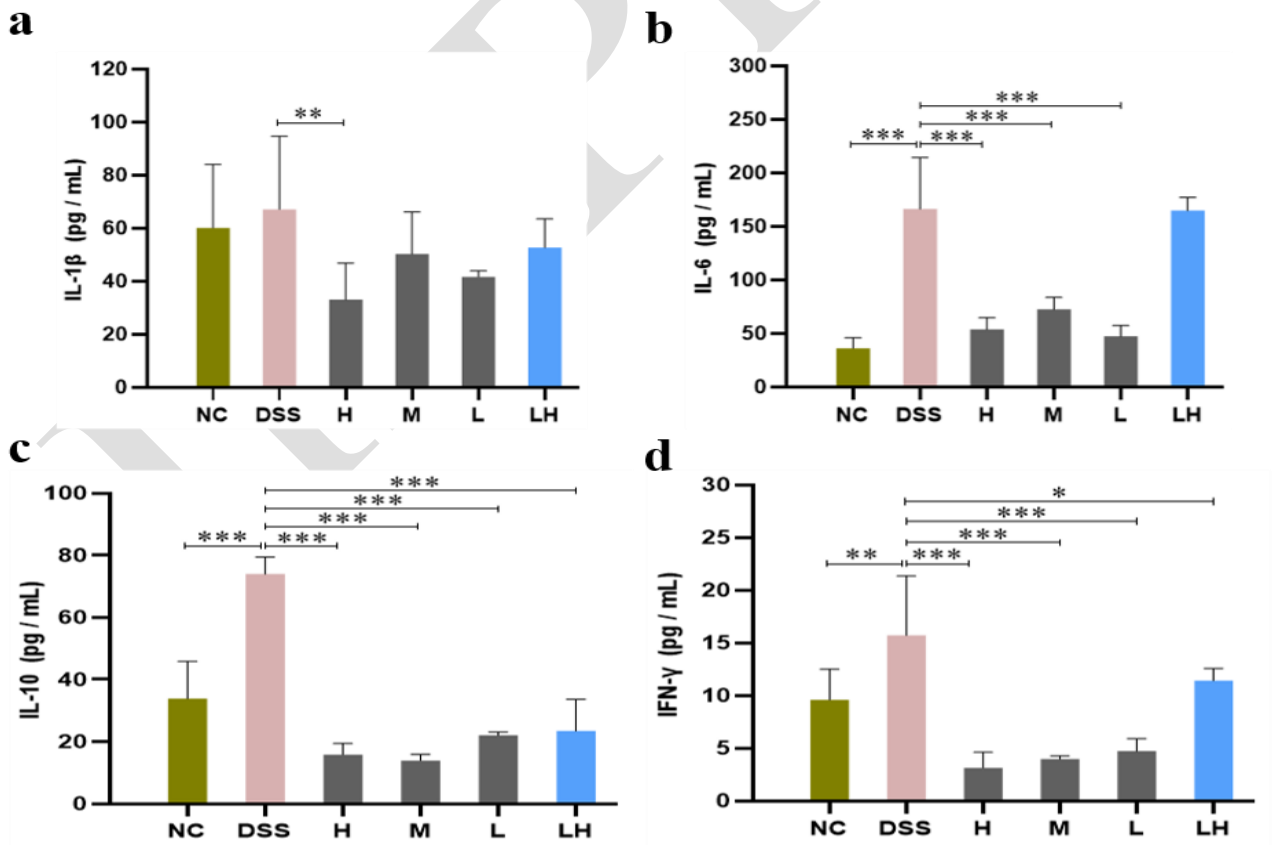

Fig. 4: The effects of AA on serum inflammatory cytokines of DSS-induced colitis mice. (a) IL-1β; (b) IL-6; (c) IL-10; (d) IFN-γ. The values are presented as mean±SD. The levels of significance are indicated as; *P<0.05, **P<0.01, and ***P<0.001.

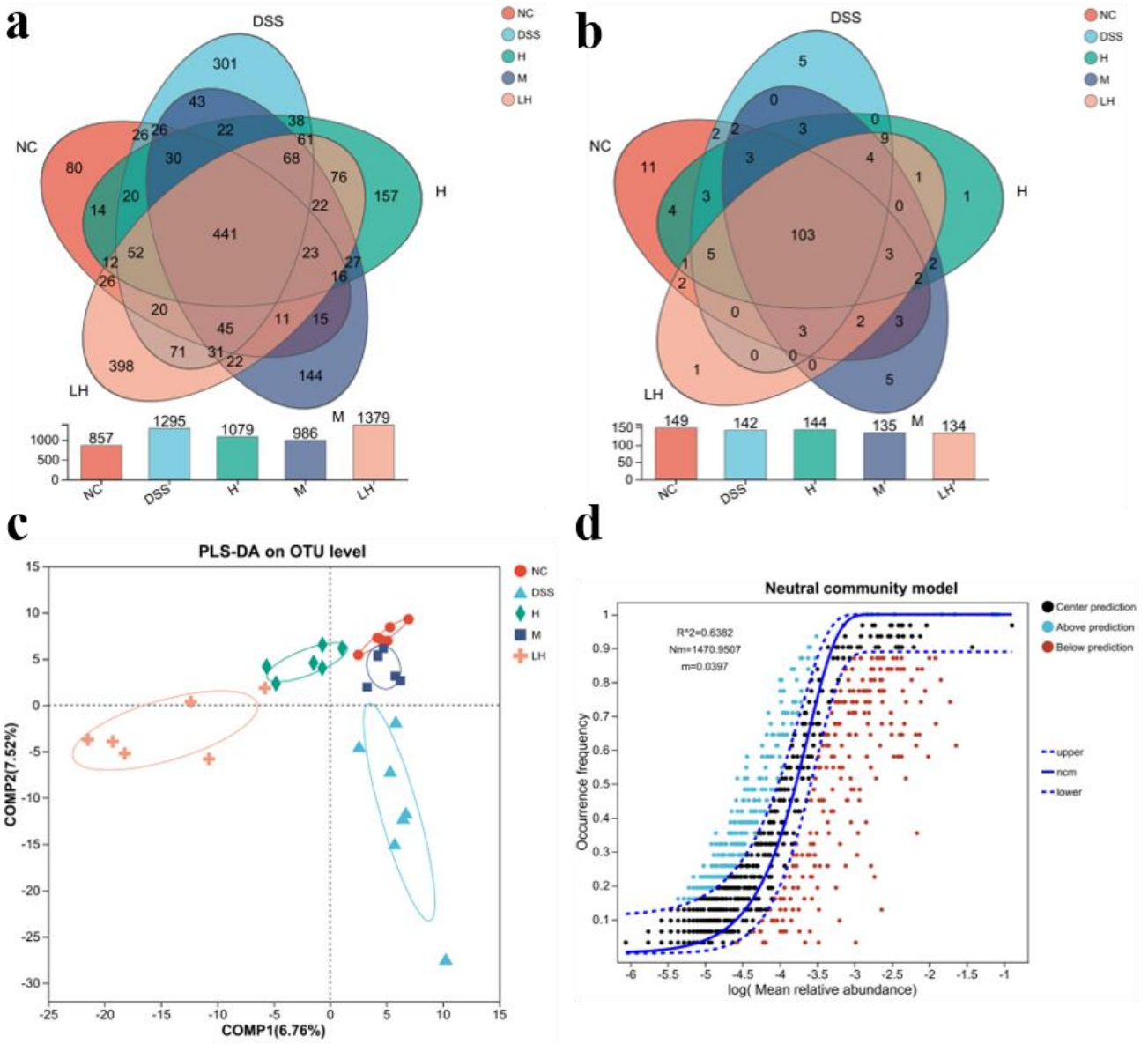

Fig. 5: Effect of AA on gut microbiota composition and structure in DSS-induced colitis mice. (a) Venn diagram showing the number of unique and shared Operational Taxonomic Units (OTUs) among groups. (b) Venn diagram at the genus level. (c) Partial Least Squares-Discriminant Analysis (PLS-DA) plot demonstrating distinct clustering of gut microbial communities. The NC, H, and M groups cluster closely, indicating a restored microbial profile. (d) Neutral Community Model (NCM) analysis. The solid red line represents the best fit, and the dashed red lines indicate the 95% confidence interval. The high R^2 value (63.82%) indicates community assembly is primarily governed by stochastic processes.

AA modulates gut microbiota and enriches beneficial bacteria: The effect of AA on gut microflora composition in mice stimulated by DSS (Fig. 6a & 6b). At the phylum level, the top predominant bacteria groups were Firmicutes, Bacteroidota, Patescibacteria, Actinobacteriota, Desulfobacterota, Campilobacterota, Proteobacteria, and *Deferribacterota*, account for more than 95% of mice gut microbiota. The RA of Firmicutes in M group was significantly greater than other groups. Compared with the DSS model group, the RA of Bacteroidota, Patescibacteria, *Deferribacterota*, and Cyanobacteria in the H and LH groups was significantly increased (Fig. 6a). At the genus level, 28 genera with RA higher than 1% were the dominant strains. The study indicated that after 3 days of treatment with AA, it can improve the RA of advantageous bacteria like *Lactobacillus*, Muribaculaceae, Ruminococcaceae, Clostridia, and Bacteroides. The RA of *Alistipes*, Oscillospirales, and *Lachnospiraceae* groups were also observed. The RA of *Candidatus_Saccharimonas* was reduced. By promoting the proliferation of beneficial bacteria, the damage degree of enteritis induced by DSS in mice was improved (Fig. 6b).

AA treatment drives distinct microbial clustering and enriches signature taxa: Circos analysis revealed that at the phylum level, the composition and percentage of predominant species in different groups varied significantly. The composition of predominant species in samples of distinct groups was similar, and the phylum-level predominant bacteria were as follows: Firmicutes, Bacteroidota, Patescibacteria, Actinobacteriota, and Desulfobacterota. Firmicutes had the lowest abundance in LH group (16%) and the highest abundance in M group (25%). The abundance of Bacteroidota was higher in the H group (31%) and LH group (37%). Patescibacteria and Actinomycetes had the highest abundance ratio only in the

NC group (46% and 55%), which was the dominant species in the NC group. Desulfobacterota was among predominant species in DSS model group with abundance of 32% (Fig. 7a-c). Principal coordinate analysis (PCoA) showed that the β diversity among samples in the 5 groups were better, and the sample points were far away, indicating that the microflora structure and composition were not similar among the groups, and the differences were obvious (Fig. 7d, p=0.001). The cumulative contribution of x-axis (28.43%) and y-axis (22.47%) reached 50.90%, indicating that different drug treatments could explain the different composition of microbial community structure among samples of each group.

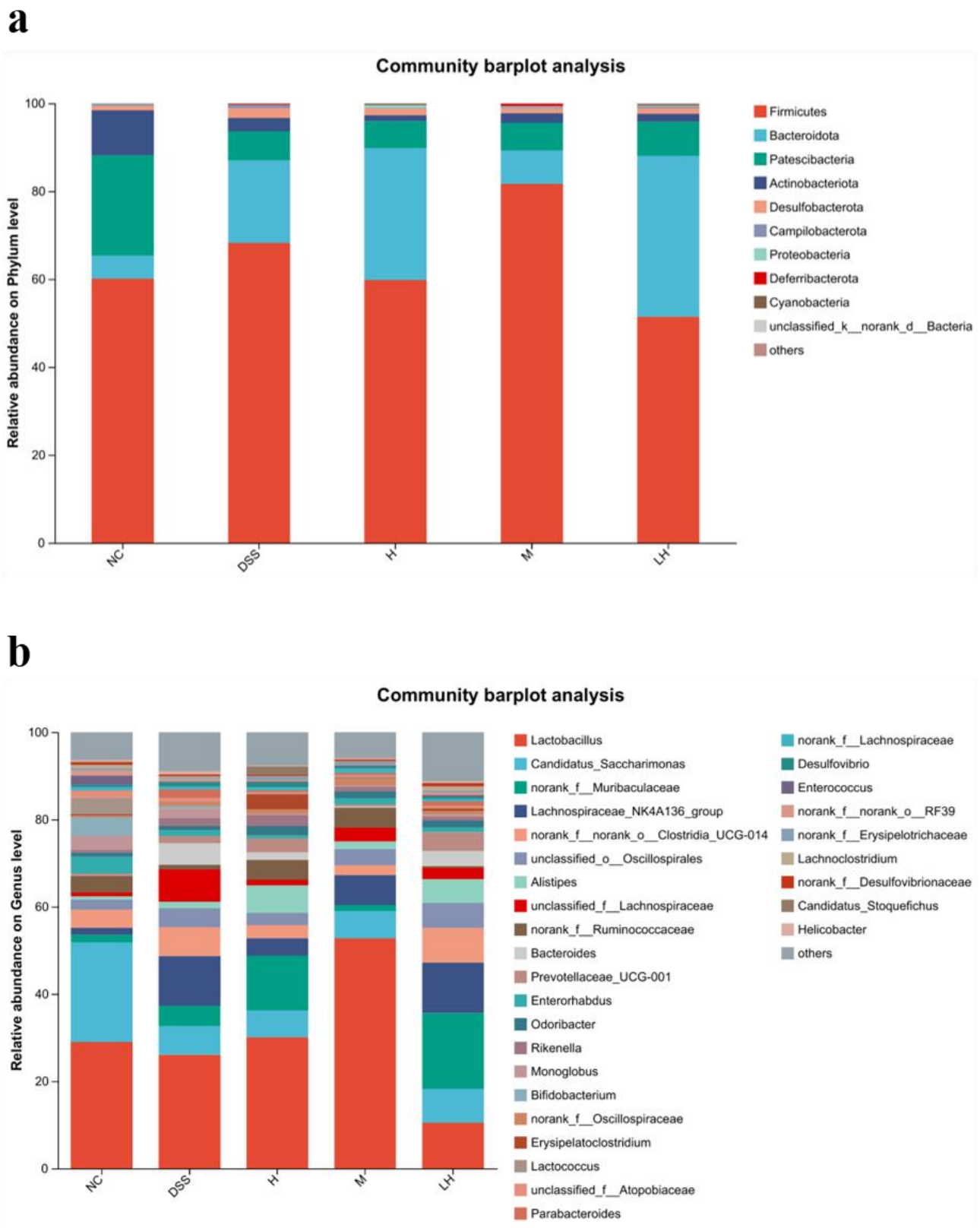

Fig. 6: Effect of on AA on gut microbiota composition at the phylum and genus level. (a) RA of the dominant bacterial phyla across experimental groups. (b) RA of the dominant bacterial genera.

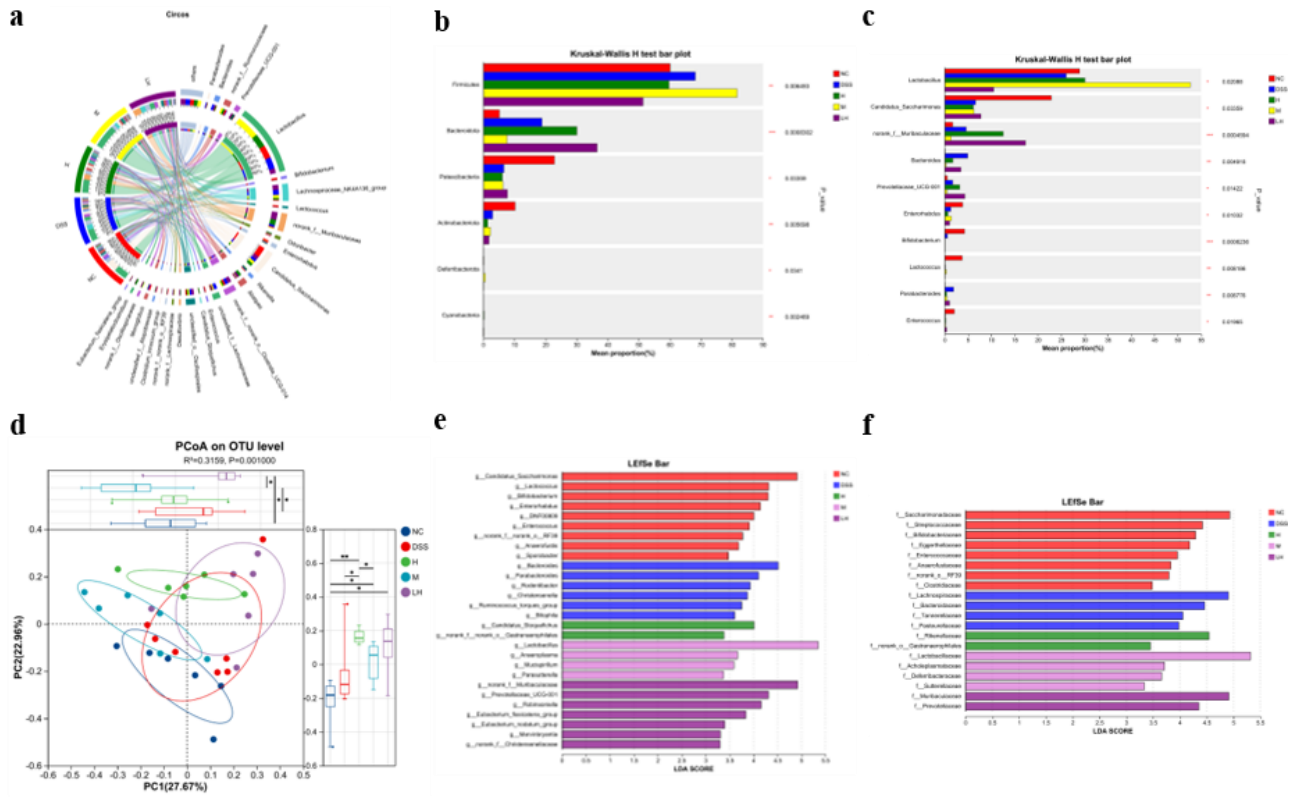

Fig. 7: Effect of AA on distinct structural shifts and enriches specific microbial taxa. (a) Circos plots visualizing the RA and distribution of the top five dominant bacterial phyla across sample groups. (b) Differential abundance of gut microbiota at the phylum level (c) Differential abundance of gut microbiota at the genus level. (d) Principal Coordinate Analysis (PCoA) plot based on Bray-Curtis dissimilarity, showing significant separation of microbial communities among groups (p=0.001). (e) Linear Discriminant Analysis (LDA) scores, identifying the specific bacterial genera. (f) LDA scores, identifying the specific bacterial families.

According to the above analysis, significant differences in microbial community structure were determined among the samples of each group. Another main purpose of comparing microbial community differences was to identify significant different species between the groups, for which linear discrimination analysis size effect (LEfSe) was used. In this study, LDA>3.5 was used as the screening criterion to identify the microorganisms with high abundance in each group. The differences in intestinal flora abundance caused by DSS-induced treatment at different species classification levels were analyzed and compared using LEfSe (Fig. 7e), and the LDA histogram of LEfSe analysis (Fig. 7f). At family and genus levels, in the NC group, f Saccharimonadaceae, f_Bifidobacteriaceae, f_Streptococcaceae, g_*Bacteroides*, g_*Parabacteroid*, and g_*Ruminococcus*, were found to be of the highest significance. While the most significant ones in DSS groups were f_Lachnospiraceae, f_Bacteroidaceae, f_Tannerellaceae, g_*Candidatus*_Saccharimonas, g_*Bifidobacterium*, g_*Lactococcus*, and g_*Enterorhabdus*. After three days of drug treatment, f_Rikenellaceae, f_Lactobacillaceae, f_Acholeplasmataceae, g_*Candidatus; Stoquefichus*, g_*Lactobacillus*, g_*Mucispirillum*, g_*Anaeroplasma*, and g_*Anaerovorax* genus are the characteristic microbial genera in H and M group. The most significant characteristic microbial genera in LH group were g_norank_f_Muribaculaceae, g_norank_f_Muribaculacea, f_Prevotellaceae, g_Prevotellaceae_UCG-001, g_Eubacterium_fissicatena_group, g_*Robinsoniella*, and g_unclassified_f_Prevotellaceae (Fig. 7e & 7f).

Phylogenetic analysis reveals group-specific microbial lineages: Phylogenetic tree constructed based on maximum likelihood method revealed that the species belong to eight phyla at order level, and the proportion of Lactobacillales belonging to Firmicutes was higher in the M group; and the proportion of Lachnospirales in DSS group and LH group was higher. Lactobacillales (Firmicutes) and Saccharimonadales (Patescibacteria) accounted for a higher proportion in the NC group (Fig. 8).

Network analysis reveals a highly interconnected microbial community with defined hubs: The degree and nodes weight can reflect the importance of species or sample nodes in the network. This study analysis showed that there were 95 species nodes with connectivity >20 at genus level, accounting for 52.78% (95/180) of the total nodes (Fig. 9a). The results of sample nodes at genus level revealed that the connectivity of nodes in the DSS model group, NC group, H group, and LH group was >90, and the connectivity of nodes in the M group was significantly different, ranging from 69 to 106. In addition, the top 50 species with total abundance in genus and species were designated for correlation networks analysis. Spearman correlation coefficient among species were calculated to analyze the relationships among the microbial dominant species in gut contents of mice in each group. The single-factor correlation network at the genus and species level reveals (Fig. 9b & 9c) that there were significant interactions among different species in the intestinal flora of mice, but the degree of correlation was different.

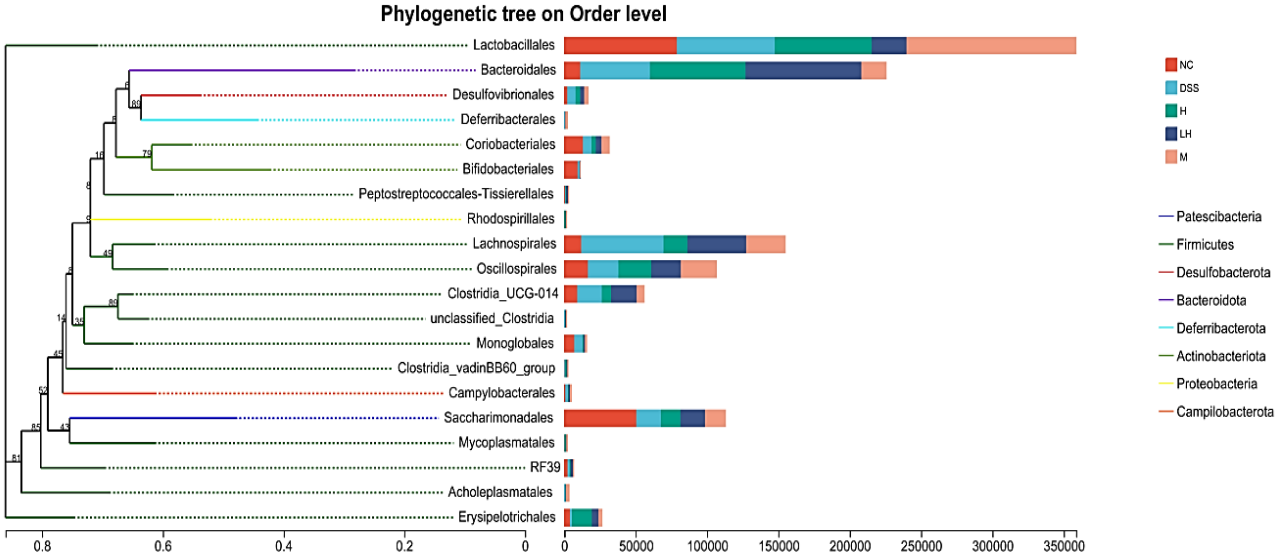

Fig. 8: Phylogenetic structure and relative abundance of gut microbiota at the order level. Branch colors represent higher-level taxonomic phyla, and branch lengths correspond to evolutionary distance. The adjacent bar plot (right) displays the RA (proportion of reads) of each species within the different experimental groups, revealing distinct group-specific microbial profiles.

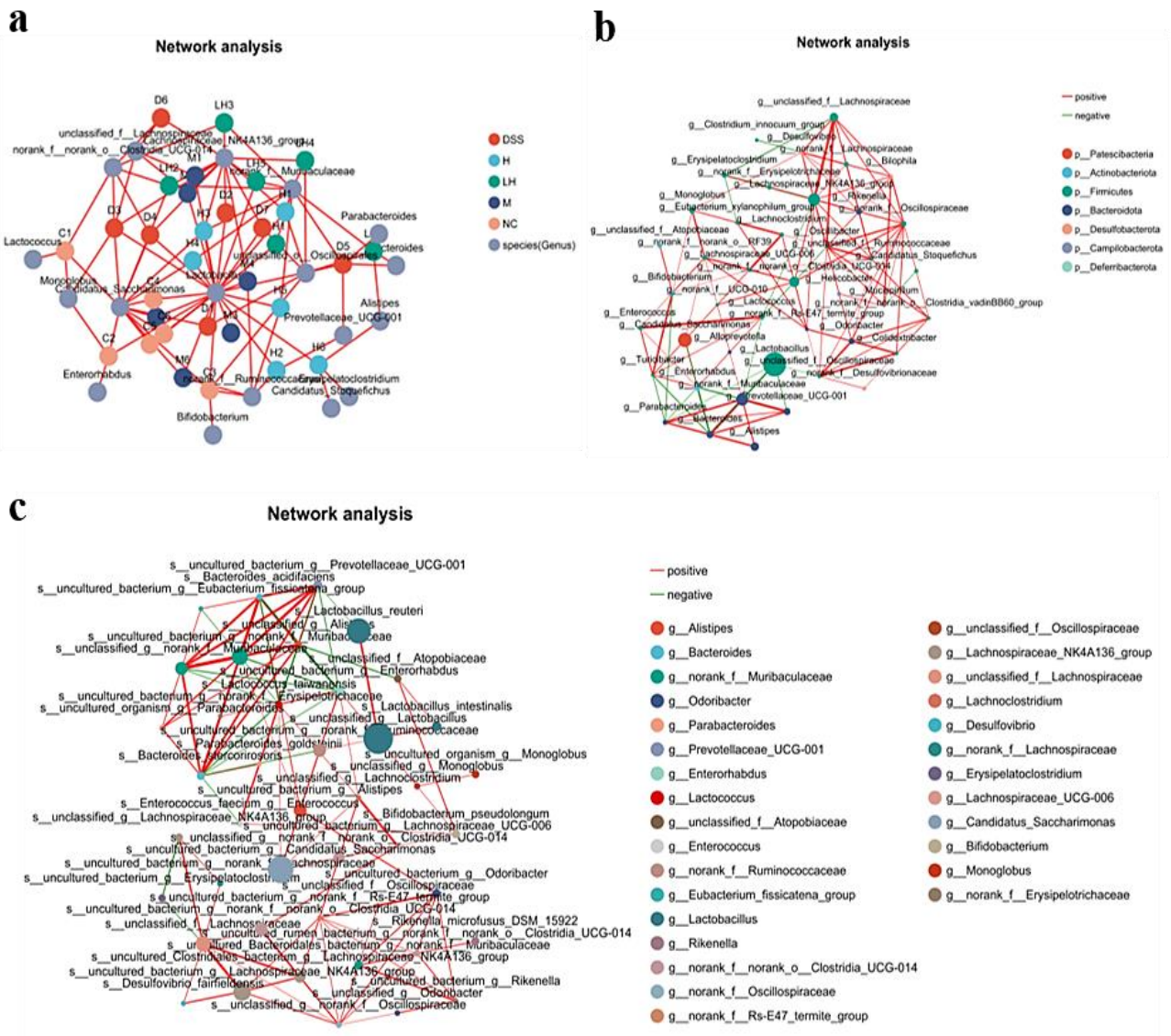

Fig. 9: Microbial co-occurrence networks and connectivity. (a) Distribution of node connectivity (degree) at the genus level. (b, c) Correlation networks illustrating significant positive (green) and negative (red) interactions between the top 50 (b) genera and (c) species. The green line represents positive correlation, the red line represents negative correlation, and the thickness of the line represents the size of the correlation coefficient.

According to the coefficient value, 98 of the 119 bacteria were positively correlated and 21 were negatively correlated at the genus level, 12 important nodes with clustering coefficient >0.5 are found by clustering value; 86 of the 104 bacteria were positively and 18 were negatively correlated at the species level, 22 important nodes with clustering coefficient greater than 0.5 are found by clustering value.

DISCUSSION

Colitis is a chronic disease of small animals that contributes potential threat to animal health. The specific pathogenesis is still unclear and control is difficult due to multiple factors such as immune, genetic, environmental, and microbial imbalance. Artemisinin (ART) and artemisinic acid (AA) are sesquiterpenoids produced from *Artemisia annua* L. They share some similarities such as part of biosynthetic pathway and derived from same terpene precursor. However, ART contains endoperoxide bridge (—O—O—) while AA contains carboxylic acid group. Moreover, AA act as synthetic precursor of artemisinin and has good water solubility than ART. As a synthetic precursor of ART, AA has a good synergistic effect on the antimicrobial activity of artemisinin, repair of intestinal damage, and reduction of diarrhea symptoms. Multiple studies have indicated that the occurrence and establishment of colitis is closely linked with intestinal flora imbalance. Therefore, this study further explored the effect of AA on DSS-induced acute colitis in mice model and its effect on intestinal microbiota.

The development of colitis is often accompanied by increased inflammation. Once the mucosal barrier is damaged, the intestinal epithelium releases inflammatory cytokines, induces neutrophils to assemble at the site of inflammation, and stimulates the intestinal epithelium to secrete large amounts of water and electrolytes, resulting in excessive inflammation (Forster *et al*., 2022). These findings showed that AA and LH could hinder the release of inflammatory cytokines IL-1β, IL-6, IL-10 and IFN-γ after DSS modeling ($P<0.01$), reduce the penetration of inflammatory mediators, maintain intestinal water balance and electrolyte metabolism to repair intestinal barrier function, and improve the repair and healing of injured tissues.

There is an extensive balance among host and intestinal microbiota, and the loss of barrier function caused by colon tissue injury is often accompanied by structural changes in intestinal flora (Huang *et al*., 2022). As per our knowledge, no studies have investigated the regulatory effects of AA on intestinal flora structure in colitis mice from the perspective of intestinal flora. In this study, through the species composition, species differences, and sample comparison analysis based on high-throughput 16S rRNA sequencing revealed that AA had a great impact on the diversity of gut microflora in mice. Bacteroidota and Firmicutes were the dominant at phylum level among the gut microbiota in all treatment groups, of this study which in accordance that these two phyla are the dominant phyla of normal animal intestinal phyla (Alioui *et al*., 2024). Previously studies have shown that Desulfobacterota may release LPS into the intestine, causing inflammation and disturbing intestinal energy metabolism at the same time (Wu *et al*., 2021) which is consistent with our findings that it's abundance was found higher in DSS group and decreased in the treatment group. LH is effective for symptom (diarrhea) control, it does not restitute a healthy microbiome, whereas AA does. This can be a compelling argument for AA's potentially superior mechanism in relieving colitis.

Based on network attributes, key species in the process of environmental change can be found, which is convenient to understand the interaction between dominant species. Through the species abundance analysis between different samples, the similarity and difference between samples can be highlighted, which is a very effective way for large and complex data (Ma *et al*., 2020). This study establishes a correlation between AA treatment and beneficial changes in the microbiome. However, it does not prove causation which is one of the limitation of this study and suggest future studies either the microbial changes were a direct effect of AA on bacteria or an indirect effect of the improved intestinal environment.

Conclusions: The study concluded the multidimensional effects of artemisinic acid (AA) on dextran sodium sulfate (DSS) induced acute colitis in mice model. The findings of this study proved that AA can alleviate colitis through regulation of inflammation and gut microbiota. This study noted that AA reduced the colitis by improving the disease activity index (DAI), increase in body weight, and maintaining the colon morphology. This study also found that AA significantly reduced the concentration of pro-inflammatory cytokines in the serum and decreased the pathological damage of colon tissue. Furthermore, AA significantly promoted the abundance of beneficial microbes such as *Lactobacillus* while suppressing the harmful microbes. Our results suggested that AA could be a potential compound to treat the colitis in animals. This study thus suggests follow up trials on fecal microbiota transplantation (FMT) to directly test if the AA modulated microbiome is sufficient to confer protection.

Ethical approval: This study was approved by the Experimental Animal Ethics Review Committee of the Lanzhou Institute of Husbandry and Pharmaceutical Sciences of the Chinese Academy of Agricultural Sciences (Permit No. LIHPS-2023-011).

Competing interests: The authors declare that they have no competing interests.

Data availability: The raw sequencing data of this study has been deposited in the NCBI database under the accession ID: PRJNA1357877.

Funding: This research was supported by Science and Technology Planning Project of Lanzhou (2023-1-4); Natural Science Foundation Project of Gansu Province (grant No. 24WY5N643); Longyuan Youth Innovation and Entrepreneurship talent project of Gansu Province (grant No. 2023LQD03); Key Research and Development Projects in Gansu Province (grant No.21YF5NA143); Agricultural Science and Technology Innovation Program

of Chinese Academy of Agricultural Sciences (grant No. CAAS-ASTIP-2014-LIHPS-04, 25-LZIHPS-03).

Authors' contributions: Conceptualization, LW, XHZ, MS, and JH; methodology, LW and XZ; software, LW, MS, and XQZ.; validation, LW, XHZ, and YY; formal analysis, LW, XHZ, YY, and WG; investigation, XHZ and XQZ; resources, LW and JH; data curation, LW, AIA, and MS; writing-original draft preparation, LW, SA, and MS; writing-review and editing, LW, AIA, and MS; supervision and project administration, LW, JH, and SW. All authors have read and agreed to the published version of the manuscript.

Acknowledgements: We thank the MajorBio Bio-Pharm Technology Co., Ltd. (Shanghai, China) for 16S rRNA sequencing and providing platform for data analysis.

REFERENCES

Addissouky TA, 2025. Artemisinin and its derivatives throughout the therapeutic mechanisms and clinical potential. Dis Chem 2: 10.

Ain QT, Saleem N, Munawar N, *et al*., 2024. Quest for malaria management using natural remedies. Front Pharmacol 15: 1359890.

Alioui Y, Ullah H, Ali S, *et al*., 2024. Polysaccharides derived from golden mushroom (*Cantharellus cibarius* Fr.) modulate gut microbiota and enhance intestinal barrier function to ameliorate dextran sulfate sodium-induced colitis in mice. Front Pharmacol 15: 1498625.

Forster SC, Clare S, Beresford-Jones BS, *et al*., 2022. Identification of gut microbial species linked with disease variability in a widely used mouse model of colitis. Nat Microbiol 7: 590-599.

Froushani SMA, Hasani SJ, Ghaderi M, *et al*., 2025. A review of inflammatory bowel diseases in humans and pets: treatment strategies. Vet Res For 16(11): 601-610.

Huang SY, Xu P, Hong ZY, *et al*., 2022. Experimental study on improvement of bacterial enteritis and regulation of intestinal flora in mice by punicalagin. Chin Trad Herb Drugs 53: 3044-3052.

Huang X, Jiang F, Chen X, *et al*., 2024. Plant-Derived Polysaccharides Benefit Weaned Piglets by Regulating Intestinal Microbiota: A Review. J Agric Food Chem. 72: 28225-28245.

Johnson JS, Spakowicz DJ, Hong BY, *et al*., 2019. Evaluation of 16S rRNA gene sequencing for species and strain-level microbiome analysis. Nat Commun 10: 5029.

Liao Y, Wang YT, Luo XQ, *et al*., 2021. Research progress on activation mechanism of artemisinin compounds in antitumor effects. *Chin Tradi Herb Drugs* 52: 3429-3435.

Liu JL, Gao YY, Zhou J, *et al*., 2020. Changes in serum inflammatory cytokine levels and intestinal flora in a self-healing dextran sodium sulfate-induced ulcerative colitis murine model. Life Sci 263: 118587.

Luo Y, Fu S, Liu Y, *et al*., 2024. Banxia Xiexin decoction modulates gut microbiota and gut microbiota metabolism to alleviate DSS-induced ulcerative colitis. J Ethnopharmacol 326: 117990.

Ma J, Wu D, Xu C, *et al*., 2025. Lactobacillus salivarius alleviated dextran sulfate sodium (DSS)-induced colitis in mice by mitigating oxidative stress and inflammatory responses through modulation of the intestinal flora. Microb Pathog 205: 107696.

Ma Y, Hu C, Yan W, *et al*., 2020. Lactobacillus pentosus increases the abundance of akkermansia and affects the serum metabolome to alleviate DSS-Induced colitis in a murine model. Front Cell Dev Biol. 8: 591408.

Ul Haq S, Wang L, Guo W, *et al*., 2022. Enhancing activity of β-lactam and fluoroquinolones antibiotics by artemisinin and its derivatives against MDR *Escherichia coli*. Front Vet Sci 9: 1048531.

Wang L, Guo W, Haq SU, *et al*., 2021. Anticoccidial activity of Qinghao powder against *Eimeria tenella* in broiler chickens. Front Vet Sci. 8: 709046.

Wang X, Ding Y, Zhang X, *et al*., 2025. The effects of degraded polysaccharides from Acanthopanax senticosus on growth, antioxidant and immune effects in broiler chicks based on intestinal flora. Poult Sci 104: 104933.

Wei K, Wei Y, Wang Y, *et al*., 2023. Amelioration effects and regulatory mechanisms of different tea active ingredients on DSS-induced colitis. J Agric Food Chem 71: 16604-16617.

Wu Z, Huang S, Li T, *et al*., 2021. Gut microbiota from green tea polyphenol-dosed mice improves intestinal epithelial homeostasis and ameliorates experimental colitis. *Microbiome 9:* 184.

Xie Q, Zhang Y, Zhang Z, *et al*., 2024. Characteristics and Dynamic Changes of Gut Microbiota in Cats with Colitis. Pak Vet J 44(2): 414-422.

Zhang L, Wang X and Zhang X, 2022. Modulation of intestinal flora by dietary polysaccharides: a novel approach for the treatment and prevention of metabolic disorders. Foods 11: 2961.

Zhu Y, Lu S, Cidan Y, *et al*., 2025. Protective effects of traditional chinese herbal medicine formulas (tchmfs) via influencing anti-oxidative capacity, inflammatory mediators, and gut microbiota in weaned yaks. Pak Vet J 45: 184-194.